Design and Experimental Investigation of a Three-Phase APF based on Feed-Forward plus Feedback Control

YANG HAN, MANSOOR, GANG YAO, LI-DAN ZHOU, CHEN CHEN
Department of Electrical Engineering
Shanghai Jiaotong University
218# XinShangYuan, 1954 Huashan Road, Xuhui District, Shanghai
CHINA
hanhansjtu@yahoo.com

Abstract: - An effective control scheme for three-phase three-wire active power filter is proposed in this paper. Conventionally, the majority of existing APF control strategies in literature adopts feed-forward control scheme, which results in switching notches (sharp-rising or falling ripples) in the source-side currents at conduction instants of diode/thyristor rectifier load. The proposed method utilizes feedback control plus feed-forward control structures to achieve a smooth filtering performance. The feedback loop minimizes the steady-state error using two separate PI regulators in d-axis and q-axis respectively. The feed-forward loop serves the purpose of load disturbance rejection and it significantly enhances performance of active power filter by using synchronous frame adaptive neural network (SADALINE) algorithm. The proposed method overwhelms many existing compensation schemes in terms of simplicity, robustness and ease of implementation using DSP. The effectiveness of the proposed control scheme has been substantially confirmed by experimental results.

Key-Words: - harmonic contamination, active filter, power quality, SADALINE

1 Introduction

The increasing application of power electronic equipment, which generates harmonic current components and severely affects the power quality of electric power distribution systems, resulting in higher distortion levels throughout the system. In recent years, power converters are widely utilized in electronic equipment, e.g., variable ac motor drive systems, HVDC systems, arc furnaces, renewable electric power generators and household appliances. The increased harmonic contamination causes an increase in line losses, instability, and voltage distortion when harmonics travel upstream and produce drop across the line impedance, which corrupts the power distribution systems. The attractive solution for all the aforementioned problems can be realized by a shunt APF [1].

The performance of APF is highly dependent on how the reference signals are generated and how the current-control is implemented. In the recent publications, J. A. R. MAC ÍAS *et al.* [2] compared Kalman filters and STDFT for harmonic estimation, it was found that STDFT method was inaccurate with the presence of decaying dc component, and Kalman filter was sensitive to un-modelled harmonic components. G. W. Chang *et al.* [3] proposed an optimization-based solution algorithm to determine the three-phase three-wire APF current injections to meet different constraints with an optimal filter size, where the voltage compensation-based control strategy is formulated as a nonlinear programming problem and is solved to find the optimal compensator gains and APF injections. However, this algorithm is rather complicated and requires great computational resources, which impedes its real-time harmonic compensation. A. M. Rios *et al.* [4] proposed a method uses a least-squares curve fitting and a phase-lock technique that allows sinusoidal and symmetrical reference voltages to be supplied to obtain the reference currents, thus the source currents are in phase with source voltages. T. Kilić *et al.* [5] proposed a predictive FIR filter-based current reference generation method. V. M. Moreno *et al.* [6] proposed a modified Fryze, Buchholz and Depenbrock (FBD) method based on a new definition of conductance for shunt APF controllers in case of nonlinear loads and non-sinusoidal grid voltages which minimize the line current distortion.

The algorithms presented in [4]-[6] seem attractive for their simplicity and ease of implementation, however, they were lack in providing adequate solutions under extreme or severe conditions of harmonics, reactive power and unbalance or their combinations with limited power rating of voltage source inverter (VSI), employed as APF, if the reference signals saturated, the APF become a source of harmonic generator itself,

further, the disturbance of fast-varying nonlinear load were un-modelled, hence these algorithms are less suitable for compensation of fast varying nonlinear loads.

Neural network based control schemes for active filters have also received considerable attention in recent years. F. Temurtas *et al.* [7] proposed the methods using the feed-forward and Elman's recurrent neural networks for harmonic detection process in active filter. However, this method is computational intensive and may loss accuracy due to model mismatch, thus difficult to be applied in practical active filter systems. K. Nishida *et al.* [8] applied adaptive neural network (ADALINE) to generate reference signals in a three-phase nonlinear load, which can not only detect the fundamental components of the load currents, but also the different higher-order harmonic components.

This paper proposes a control scheme using feedback plus feed-forward control structures. Different from the deadbeat control plus stationary frame ADALINE schemes discussed in [8], the feedback loop control is based on the decoupled state-space equations and the feed-forward loop is based on synchronous frame adaptive linear neural network (SADALINE), which mainly serves the purpose of load disturbance rejection and simplifies computational load compared to the stationary frame ADALINE used in [8]. In some discontinuous nonlinear loads like three-phase rectifier, the weights adaptation process has longer delay in stationary frame ADALINE algorithms when there is a transient in the estimated currents. By adopting synchronous frame SADALINE algorithm, its order and weights updating delay can be minimized. Thus fast convergence speed is obtained with sufficient accuracy. Owing to less computational load for the similar performance, the proposed synchronous frame ADALINE algorithm has adequate accuracy, sufficient dynamic response and better online harmonic estimation capabilities. The validity and effectiveness of the proposed schemes have been confirmed by experimental results.

This paper is organized as: Section 2 discusses mathematical model of 3-phase 3-wire active filter using state-space representations and thereby feedback control loop is formed using the decoupled state-space equations. Section 3 reviews the concept of adaptive linear neural network (ADALINE), and a comparison of weights updating process between stationary frame and synchronous frame ADALINE. Section 4 discusses experimental results using the proposed feedback control plus SADALINE-based feed-forward control schemes. Finally, section 5 concludes this paper.

2 Modelling of 3-phase 3-wire shunt Active Power Filter

Fig.1 shows the schematic of three-phase three-wire APF and its control blocks. In this section, we briefly address the mathematical models of the 3-phase 3-wire active filter. Thereby, the feedback control loop can be attained from the decoupled state-space equations.

As shown in Fig.1, the output voltages of voltage source inverter (VSI) can be derived as

$$U_{iab} = (f_1 - f_2)V_{dc}, U_{ibc} = (f_2 - f_3)V_{dc}, U_{ica} = (f_3 - f_1)V_{dc}$$

(1)

Where V_{dc} is dc capacitor voltage, f_1, f_2, f_3 are switching functions of each arm, assumed to be zero or one according to the state of each converter arm, depending on the PWM pulse patterns. The phase voltages are derived as:

$$U_{ia} = h_1 V_{dc}, U_{ib} = h_2 V_{dc}, U_{ic} = h_3 V_{dc} \quad (2)$$

Where

$$H_{123} = \begin{bmatrix} h_1 \\ h_2 \\ h_3 \end{bmatrix} = \frac{1}{3} \begin{bmatrix} 2 & -1 & -1 \\ -1 & 2 & -1 \\ -1 & -1 & 2 \end{bmatrix} \begin{bmatrix} f_1 \\ f_2 \\ f_3 \end{bmatrix}. \quad (3)$$

Assuming the switching function h_1, h_2 and h_3 are 0, $\pm 1/3$, $\pm 2/3$. The state-space equation for the voltage source inverter is obtained:

$$\begin{bmatrix} \dfrac{di_{fa}}{dt} \\ \dfrac{di_{fb}}{dt} \\ \dfrac{di_{fc}}{dt} \end{bmatrix} = \begin{bmatrix} -\dfrac{R_a}{L1} & 0 & 0 & -\dfrac{h_1}{L1} \\ 0 & -\dfrac{R_a}{L1} & 0 & -\dfrac{h_2}{L1} \\ 0 & 0 & -\dfrac{R_a}{L1} & \dfrac{h_3}{L1} \end{bmatrix} \begin{bmatrix} i_{fa} \\ i_{fb} \\ i_{fc} \\ V_{dc} \end{bmatrix} + \begin{bmatrix} \dfrac{u_{sa}}{L1} \\ \dfrac{u_{sb}}{L1} \\ \dfrac{u_{sc}}{L1} \end{bmatrix} \quad (4)$$

Where R_a is equivalent resistance of the interfacing inductance L1, and u_{sa}, u_{sb}, u_{sc} are voltages at point of common coupling (PCC).

$$C_{dq0}^{abc} = \sqrt{\frac{2}{3}} \begin{bmatrix} \cos \omega t & \cos(\omega t - \dfrac{2\pi}{3}) & \cos(\omega t + \dfrac{2\pi}{3}) \\ -\sin \omega t & -\sin(\omega t - \dfrac{2\pi}{3}) & -\sin(\omega t + \dfrac{2\pi}{3}) \\ \dfrac{1}{\sqrt{2}} & \dfrac{1}{\sqrt{2}} & \dfrac{1}{\sqrt{2}} \end{bmatrix}. \quad (5)$$

Multiplying (4) using Park's equation (5), hence state-space equation in synchronous rotating reference frame is obtained as (6):

$$\begin{bmatrix} \dfrac{di_{fd}}{dt} \\ \dfrac{di_{fq}}{dt} \end{bmatrix} = \begin{bmatrix} -\dfrac{R_a}{L1} & \omega & -\dfrac{h_1}{L1} \\ -\omega & -\dfrac{R_a}{L1} & -\dfrac{h_2}{L1} \end{bmatrix} \begin{bmatrix} i_{fd} \\ i_{fq} \\ V_{dc} \end{bmatrix} + \begin{bmatrix} \dfrac{u_d}{L1} \\ \dfrac{u_q}{L1} \end{bmatrix}. \quad (6)$$

Where u_d, u_q are PCC voltages and i_{fd}, i_{fq} are inverter currents in synchronous rotating reference frame.
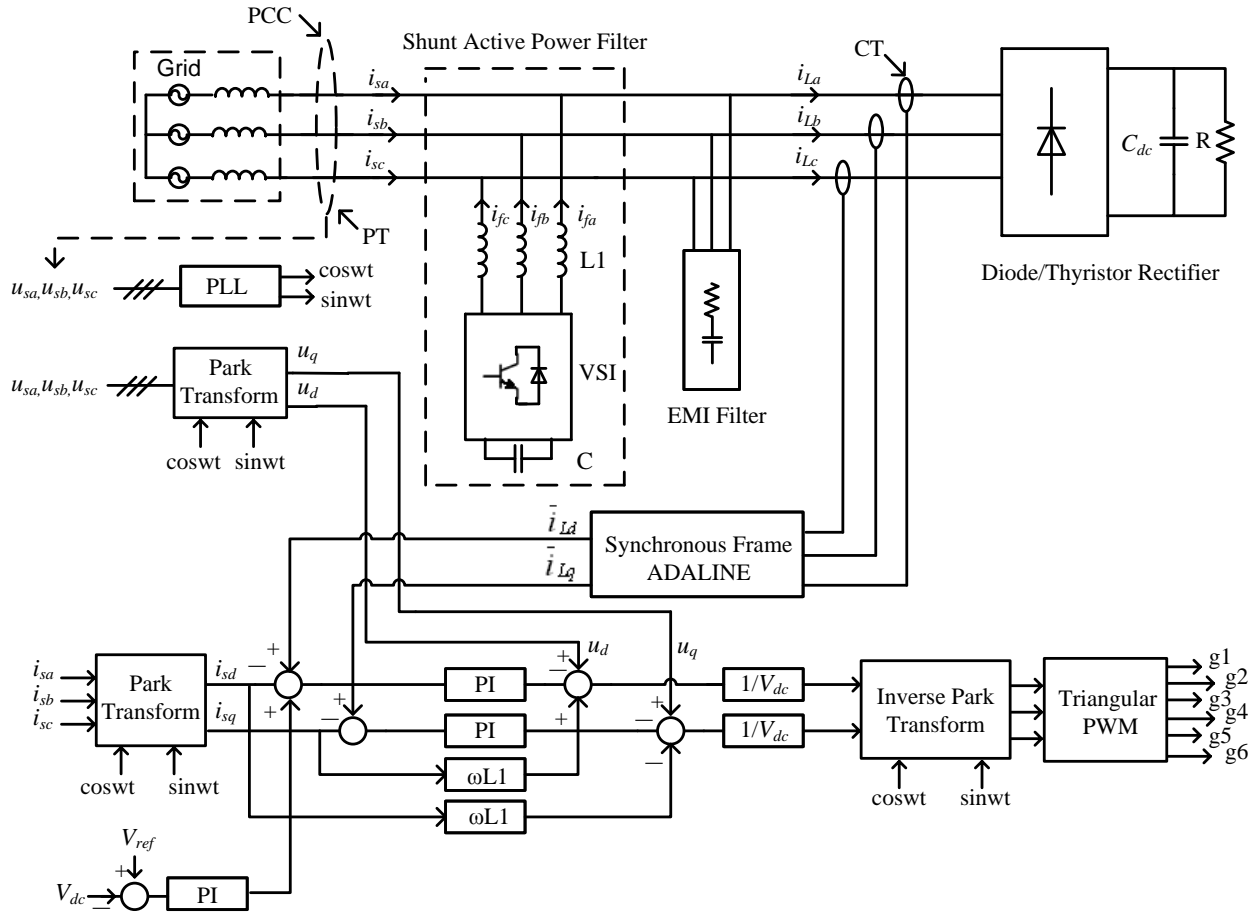
Fig.1 Schematic of proposed three-phase APF including its control scheme

According to kirchoff's law, the current of the VSI dc side capacitor satisfies the equation (7):

$$C\frac{dV_{dc}}{dt} = i_{dc} = h_1 i_{fa} + h_2 i_{fb} + h_3 i_{fc} \qquad (7)$$

Where i_{fa}, i_{fb}, i_{fc} are VSI currents in phase coordinates. Applying coordinate transformation to (7), the following equation is obtained:

$$\frac{dV_{dc}}{dt} = \frac{1}{C}\begin{bmatrix} h_1 & h_2 & h_3 \end{bmatrix}\begin{bmatrix} i_{la} - i_{sa} \\ i_{lb} - i_{sb} \\ i_{lc} - i_{sc} \end{bmatrix}$$

$$= \frac{1}{C}[C_{abc}^{dq0} H_{dq0}]^T \cdot C_{abc}^{dq0}[i_{ldq0} - i_{sdq0}] \qquad (8)$$

$$= \frac{1}{C} H_{dq0}^T \cdot [i_{ldq0} - i_{sdq0}]$$

$$= -\frac{h_d}{C} i_{sd} - \frac{h_q}{C} i_{sq} + \frac{h_d i_{ld} + h_q i_{lq}}{C}.$$

Where i_{ld} and i_{lq} are load currents in synchronous frame, C_{abc}^{dq0} represents inverse Park's transformation. The switching functions h_d and h_q are computed from h_1, h_2 and h_3 the same way as i_{sd} and i_{sq} are computed from i_{sa}, i_{sb} and i_{sc}.

Therefore, by combining (6) and (8), the complete state-space equation of the system is derived:

$$\begin{bmatrix} \dfrac{di_{fd}}{dt} \\ \dfrac{di_{fq}}{dt} \\ \dfrac{dV_{dc}}{dt} \end{bmatrix} = \begin{bmatrix} -\dfrac{R_a}{L1} & \omega & -\dfrac{h_d}{L1} \\ -\omega & -\dfrac{R_a}{L1} & -\dfrac{h_q}{L1} \\ -\dfrac{h_d}{C} & \dfrac{h_q}{C} & 0 \end{bmatrix}\begin{bmatrix} i_{fd} \\ i_{fq} \\ V_{dc} \end{bmatrix} + \begin{bmatrix} \dfrac{u_d}{L1} \\ \dfrac{u_q}{L1} \\ \dfrac{i_{dis}}{C} \end{bmatrix}. \quad (9)$$

Here i_{dis} represents the term $h_d i_{ld} + h_q i_{lq}$ in (8), which is an approximation of load dynamics, considering dc-link capacitor of VSI big enough.

$$U_d = u_d - h_d V_{dc} + \omega L_1 i_{fq},$$
$$U_q = u_q - h_q V_{dc} - \omega L_1 i_{fd}. \qquad (10)$$

Using the controller presented in (10), decoupling between d and q axis is achieved using the new inputs U_d and U_q. Thus the decoupled system model is obtained:

$$\begin{bmatrix} \dfrac{di_{fd}}{dt} \\ \dfrac{di_{fq}}{dt} \end{bmatrix} = \begin{bmatrix} -\dfrac{R_a}{L_1} & 0 \\ 0 & -\dfrac{R_a}{L_1} \end{bmatrix}\begin{bmatrix} i_{fd} \\ i_{fq} \end{bmatrix} + \begin{bmatrix} \dfrac{1}{L_1} & 0 \\ 0 & \dfrac{1}{L_1} \end{bmatrix}\begin{bmatrix} U_d \\ U_q \end{bmatrix} \quad (11)$$

Hence typical PI controllers are used to regulate the real and reactive current in synchronous frame respectively. Furthermore, the difference between the actual and the reference voltage is fed to the voltage loop controller. A separate PI controller is used to regulate dc voltage of the inverter in order to balance the active power, and the output of this controller is finally fed into the d-axis current controller (Fig.1).

A better system model can be obtained by writing the state space equations considering the load side arm, but no such effort will be made over here. Instead, a feed-forward loop based on synchronous frame adaptive neural network (SADALINE) is adopted to predict and minimize the effect of load side disturbances, which would be addressed in the next section.

3 Load-Disturbance Rejection using Synchronous Frame ADALINE

In this investigation, the synchronous frame ADALINE is utilized to estimate the dc components of load-side currents in the synchronous frame, which corresponds to positive-sequence fundamental components in stationary a-b-c frame. Then the estimated signals are applied in the feed-forward loop of the control algorithm. It was found that synchronous frame ADALINE (SADALINE) has less computational load and faster weights updating characteristics compared with stationary frame solutions [8].

The following subsections review the definition of ADALINE, and the weights updating process in stationary frame and synchronous frame are compared, which demonstrate the superior features of synchronous frame ADALINE.

3.1 Review of ADALINE

Consider an arbitrary signal *Y(t)* with Fourier series expansion:

$$Y(t) = \sum_{n=0,1,2,3,\cdots}^{N} A_n \sin(n\omega t + \varphi_n) + \varepsilon(t)$$
$$= \sum_{n=0,1,2,3,\cdots}^{N} (a_n \sin 2\pi n f t + b_n \cos 2\pi n f t) + \varepsilon(t) \quad (12)$$

Where A_n and φ_n are correspondingly the amplitude and phase angle of the nth order harmonic component, and $\varepsilon(t)$ is approximation error.

Assuming there are m samples, $(t_k, Y(t_k))$, where k=0 to m-1. The objective is to estimate the amplitude and phase of harmonics of (12) so as to find the optimum solution in the sense of least mean squares (LMS):

$$E(k) = \frac{1}{2}\sum_{k=0}^{m-1}(Y(t_k) - \sum_{n=0,1,2,3,\cdots}^{N}(a_k \sin 2\pi n f t_k + b_k \cos 2\pi n f t_k))^2$$

$$(13)$$

Assuming the estimated vector at the kth iteration is

$$W(k) = [b_{k0}, a_{k1}, b_{k1}, a_{k2}, b_{k2}, ..., a_{kN}, b_{kN}]^T \quad (14)$$

And the ADALINE input vector, *X(k)*, is chosen to be:

$$X(k) = [\sin \omega t_k \ \cos \omega t_k \ \sin 2\omega t_k \ \cos 2\omega t_k,$$
$$\cdots, \sin N\omega t_k \ \cos N\omega t_k \ ]^T. \quad (15)$$

The optimization problem is quadratic and its minimum can be found provided the Hessian matrix corresponding to the objective function is positive semi-definite. The optimum solution of (13) corresponds to the steady-state solution of the following differential equation:

$$\frac{dW}{dt} = -\mu \nabla E \quad (16)$$

Where μ is a row vector, denoting the step size of integration and ∇E is the gradient of the objective function (16), derived as:

$$\frac{\partial E}{\partial a_n} = \mu_{a_n} \sum_{k=0}^{m-1}(Y(t_k) - \sum_{n=0}^{N}(a_n \sin 2\pi n f t_k + b_n \cos 2\pi n f t_k))\sin 2\pi n f t_k$$

$$(17)$$

$$\frac{\partial E}{\partial b_n} = \mu_{b_n} \sum_{k=0}^{m-1}(Y(t_k) - \sum_{n=0}^{N}(a_n \sin 2\pi n f t_k + b_n \cos 2\pi n f t_k))\cos 2\pi n f t_k$$

$$(18)$$

Let $Y_1(t_k)$ be the output of the ADALINE, which is set to be the fundamental component of the estimated signal, then ADALINE algorithm estimates this signal by adjusting the weight vector *W(k)* recursively using Widrow-Hoff (W-H) delta rule which minimizes the average square error *E(tk)* between the measured signal *Y(tk)* and estimated signal *Yest(tk)*. The weight vector *W* for next iteration can be written as

$$W(k+1) = W(k) + \frac{\mu\varepsilon(k)X(k)}{X^T(k)X(k)}. \quad (19)$$

Where $\varepsilon(t_k) = Y(t_k) - Y_{est}(t_k)$ and $X^T(k)X(k)$ is the quadratic of the vector *X(k)*. In (19), the step size μ, also called learning rate, is used to adjust the convergence speed and improve the stability of the closed-loop updating algorithm. The performance of the weights updating process could be further optimized by using genetic algorithm (GA) [9], but a constant learning rate is considered for simplicity. When tracking error $\varepsilon(t_k)$ is minimized, the weight vector *W* after convergence would be:

$$W(k) = [b_0, a_1, b_1, a_2, b_2, ..., a_N, b_N]^T. \quad (20)$$

Obviously, the fundamental component as well as higher order harmonics can be obtained after the convergence of the neural network. An interesting

phenomenon of rectifier load currents is that, during transient condition, each phase current does not vary homogenously since the rectifier current is zero during certain parts of the cycle. Consequently, one of the three phases suffers a delay during the transient process of the estimated current, which also affects the weight updating process. Hence, in order to highlight the superior feature of applying ADALINE in synchronous rotating frame, the next subsection compares the dynamic weights updating process in stationary frame and synchronous frame.

3.2 Comparison between Stationary Frame and Synchronous Frame ADALINE
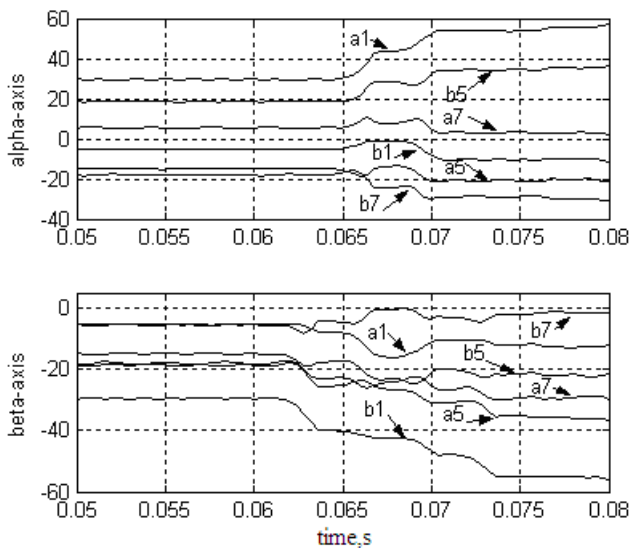
Fig.2 Weights updating process of adaptive neural network in stationary α-β frame

Fig.2 and Fig.3 show the weights updating process in stationary α-β frame and synchronous d-q frame for harmonic estimation of rectifier current, respectively. The system parameters are shown in Section 4 with a learning rate of 0.45 both for both cases, and the harmonics of the order 1,5,7,11,13,17,19 are considered for ADALINE, equivalently, the harmonics of the order 6n (n=0, 1, 2, 3) are considered for SADALINE.

The load is increased at t=0.06s to test the transient response of these algorithms. Fig.2 shows weights adaptation of α-axis has a delay of about 6ms after the transient is applied at t=0.06s, which is the worst case scenario. Fig.3 shows the delay of weights adaptation process is about 2.5ms both for the d-axis and q-axis after the transient is applied at t=0.06s. It can be deduced from Figs.2-3 that the synchronous frame SADALINE has less computational delay in weights adaptation process

compared to the stationary frame ADALINE. Therefore, the performance of SADALINE in real time computation would have better disturbance rejection capability than the stationary frame solutions. Hence the synchronous frame ADALINE is applied in the feed-forward compensation of active filer for load disturbance rejection in order to achieve a smooth filtering performance.
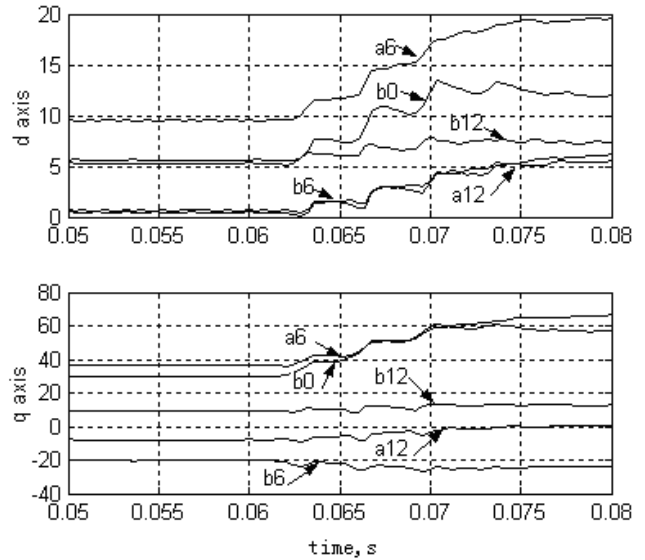
Fig.3 Weights updating process of adaptive neural network in synchronous d-q frame

4 Experimental Investigations

In order to verify the validity of the proposed compensation scheme, laboratory prototype is built, and the parameters of main circuit are: L1=200μH, C=5000μF and the dc-voltage reference of VSI is 650V, the load is 5kW thyristor rectifier. The digital signal processors (TI TMS3202812) is used as main controller and the field programmable gate array (FPGA) is used to generate PWM signals for the insulated gate bipolar transistors (IGBTs).

Fig.4 shows the rectifier load currents and PCC voltage in phase 'a' before compensation. The conduction angle of thyristor rectifier load is set to be 70 degree. After the APF is turned on, the source-side currents and PCC voltage in phase 'a' are shown in Fig.5.

It is found that the THD of phases 'a', 'b', 'c' currents are 38.5%, 34.1% and 36.4% respectively before the APF is turned on, however, when the APF is applied, the THD of each phase current deceases to below 3.5%. Further, it can be observed that the source-side currents become sinusoidal and notch-free, and the wave-shapes are quite smooth, which demonstrates the effectiveness of the proposed control schemes.
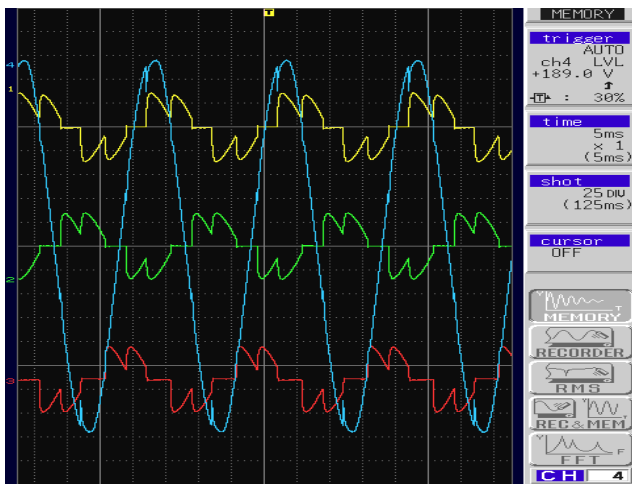
Fig.4 Rectifier load currents (marked as 1, 2, 3) and PCC voltage in phase 'a' (marked as 4) before compensation
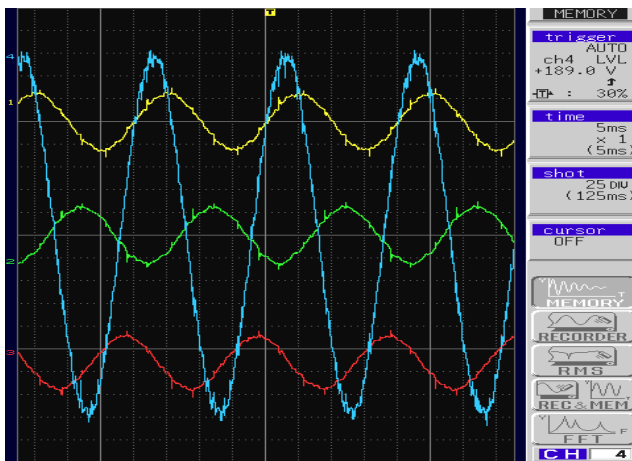
Fig.5 Source-side currents (marked as 1, 2, 3) and PCC voltage in phase 'a' (marked as 4) after APF is turned on

5 Conclusions

In this paper, an effective control scheme for three-phase active power filter is proposed, based on the feedback control plus feed-forward control structures. The feedback control minimizes the steady-state error, while the feed-forward compensation is used for load disturbance rejection by using synchronous frame adaptive neural network (SADALINE). The superior characteristics of synchronous frame ADALINE has been proven through the comparison of weights updating process between stationary frame and synchronous frame solutions. It has been found that the proposed control schemes overwhelm most of the existing methods in terms of simplicity, robustness, and ease of implementation. The effectiveness of the proposed method has been substantially confirmed by experimental results.

References:
[1] T. JAROU, M. CHERKAOUI, M. MAAROUFI, Contribution to the controlling of the shunt active power filter to compensate for the harmonics, unbalanced currents and reactive power, *Proc. WSEAS/IASME Int. Conf. on Electric Power Systems, High Voltages, Electric Machines*, Tenerife, Spain, Dec. 16-18, 2006, pp. 263-269

[2] J. A. ROSENDO MACÍAS, A. GÓMEZ EXPÓSITO, A comparison between Kalman filters and STDFT for harmonic estimation in power systems, *Proc. WSEAS/IASME Int. Conf. on Electric Power Systems, High Voltages, Electric Machines*, Tenerife, Spain, Dec. 16-18, 2005, pp. 574-578

[3] G. W. Chang, C. M. Yeh, W. C. Chen, Meeting IEEE-519 current harmonics and power factor constraints with a three-phase three-wire active power filter under distorted source voltages, *IEEE Trans. Power Del.*, vol.21, no.3, 2006, pp.1648-1654

[4] A. M. Rios, H. A. R. Carranza, An active power filter in phase coordinates for harmonic mitigation, *IEEE Trans. Power Del.*, vol.22, no.3, 2007, pp. 1991-1993

[5] T. Kilić, S. Milun, G. Petrović, Design and implementation of predictive filtering system for current reference generation of active power filter, *Electr. Power Energy Syst.,* vol.29, 2007, pp. 106-112

[6] V. M. Moreno, A. Pigazo, Modified FBD method in active power filters to minimize the line current harmonics, *IEEE Trans. Power Del.*, vol.22, no.1, 2007, pp. 735-736

[7] F. Temurtas, R. Gunturkun, N. Yumusak, H. Temurtas, Harmonic detection using feed forward and recurrent neural networks for active filters, *Electr. Power Syst. Res.,* vol.72, 2004, pp. 33-40

[8] K. Nishida, M. Rukonuzzaman and M. Nakaoka, Digital control three-phase shunt active power filter with a new harmonic-current-extraction process, *IEE Proc. –Gener. Transm. Distrib.*, vol.152, no.4, 2005, pp. 529-538

[9] M. A. ZANJANI, GH. SHAHGHOLIAN, M. B. POODEH, S. ESHTEHARDIHA, Adaptive Integral-Proportional Controller in Static Synchronous Compensator Based on Genetic Algorithm, *Proc. WSEAS Int. Conf. on Electric Power Systems, High Voltages, Electric Machines*, Venice, Italy, Nov. 21-23, 2007, pp. 40-45